

Exploring Multiple Binding Modes Using Confined Replica Exchange Molecular Dynamics

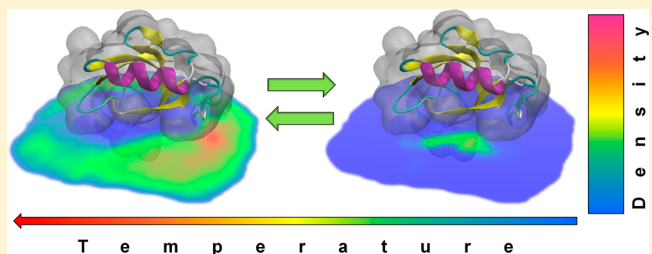
Massimiliano Anselmi^{*,†,‡} and M. Teresa Pisabarro^{*,†}

[†]Structural Bioinformatics, BIOTEC TU Dresden, Tatzberg 47-51, 01307 Dresden, Germany

[‡]Dipartimento di Scienze e Tecnologie Chimiche, Università di Roma “Tor Vergata”, Via della Ricerca Scientifica, 00133 Rome, Italy

Supporting Information

ABSTRACT: Molecular docking is extensively applied to determine the position of a ligand on its receptor despite the rather poor correspondence between docking scores and experimental binding affinities found in several studies, especially for systems structurally unrelated with those used in the scoring functions’ training sets. Here, we present a method for the prediction of binding modes and binding free energies, which uses replica exchange molecular dynamics in combination with a receptor-shaped piecewise potential, confining the ligand in the proximity of the receptor surface and limiting the accessible conformational space of interest. We assess our methodology with a set of protein receptor–ligand test cases. In every case studied, the method is able to locate the ligand on the experimentally known receptor binding site, and it gives as output the binding free energy. The added value of our approach with respect to other available methods is that it quickly performs a conformational space search, providing a set of bound (or unbound) configurations, which can be used to determine phenomenological structural and energetic properties of an experimental binding state as a result of contributions provided by diversified multiple binding poses.



INTRODUCTION

Accurate prediction of ligand–receptor binding affinities plays a crucial role in computer-aided drug design. Due to its speed and easy to use, molecular docking is still the most commonly used computational structure-based method to determine the position of a ligand on its receptor. Docking methods use diverse scoring functions and are able to predict binding modes with reasonable accuracy and distinguish between binders and nonbinders in a large set of ligand–receptor systems (i.e., virtual screening). However, the prediction of the binding affinity is still a challenging task.^{1–4} The low success rate of docking in predicting the binding affinities correctly may reside in part in the rigidity of the receptor and, when included, in the proper consideration of structural water molecules. In fact, during most commonly applied docking procedures, both the receptor and the solvent molecules, if included at all, are mostly kept fixed, whereas only the ligand is treated flexible. Nevertheless, a number of commonly used docking software packages implement features that allow the introduction of some flexibility either in the binding site or receptor surface, or options for using an ensemble of protein structures, despite the higher computational cost involved.^{5–9} Notwithstanding, current implementations do not allow for adequately modeling the conformational changes induced by the ligand on its receptor. Even more importantly, the scoring functions used do not consider the possibility that multiple binding poses might contribute to the overall affinity of the ligand. This effect is particularly critical in the case of reasonably extended, and

relatively flexible ligands (i.e., containing several dihedral angles with certain rotational freedom), or in cases in which the ligand does not adopt a defined restricted conformation, or when the binding site is not an exact footprint of the ligand, allowing the latter for a significant mobility. Typical cases for such scenarios are peptides or oligosaccharides in interaction with protein domains not presenting a well-defined deep cleft as binding site but instead offering surface patches as binding regions. In such latter cases, ligands can occupy a set of even slightly different positions on the receptor surface, and, for each of such positions, they could still adopt several conformations and orientations. Even if not all of these binding modes maximize the interaction with the receptor (leading to enthalpically favored complexes), they could, however, give a considerable entropic contribution to the overall ligand affinity.

When the geometry of the bound ligand is known, different classes of methods can be used to predict the binding affinities: free energy perturbation, thermodynamic integration,^{10–14} linear interaction energy,^{15–18} MM/PBSA,¹⁹ umbrella sampling/weighted histogram analysis method,²⁰ steered/force probe MD,^{21,22} and their variations. Such methods can greatly increase the accuracy of binding affinity predictions. The improved accuracy of the simulations is mainly due to the increased level of molecular detail, the consideration of flexibility, and the inclusion of a more adequate solvation

Received: March 17, 2015

model. However, the much more elaborated nature of such procedures and the consequently increased simulation time needed for each system substantially limits their application. Furthermore, challenges also originate by considering a limited number of initial structures (i.e., provided by molecular docking or experimentally obtained), which precludes sufficient enhancement of the sampling and, thus, does not allow for adequate prediction of the entropic contribution to binding affinity.

Docking and scoring calculations can be performed by applying molecular dynamics (MD) and Monte Carlo (MC) techniques, when based on a reasonably accurate force field and including solvation effects. In principle, such approaches should find the right bound geometry of ligand and receptor and to accurately predict their binding affinity. Unfortunately, this often turns out to be not feasible, since the simulation time period is much shorter than the time necessary for the real binding process. For this reason, in the field of molecular docking, MD simulations are applied linked to some other methods aimed to sample the conformational space efficiently. Several approaches based on MD or MC methods have been adopted to study receptor–ligand binding modes. Di Nola and Berendsen²³ were pioneers in using molecular dynamics in explicit water to address the docking of two flexible molecules. MD docking (MDD)^{23,24} consists of a separation of the center-of-mass motion of the ligand from its internal and rotational motions and a consequent coupling to different thermal baths. In this manner, the high temperature of the center-of-mass prevents the system from getting trapped in an energy local minimum, allowing control of the search rate without disturbance of the ligand internal structure. Wang and Pak²⁵ applied a new MD method to flexible ligand docking using a well jumping technique, where a scaling function is applied to the equations of motion to facilitate barrier crossing by effectively reducing the magnitude of the forces. Likely, multicanonical molecular dynamics addresses the problem of limited conformational sampling and was used as a technique to dock flexible ligands by Nakajima et al.²⁶ Wenzel and co-worker addressed the same problem by means of parallel tempering²⁷ and stochastic tunneling methods.²⁸ Fukunishi et al. proposed the filling potential (FP) method²⁹ utilizing umbrella sampling in combination with the Taboo search algorithm³⁰ that consists of sequential searches of the local minimum and the saddle points. Parrinello and co-workers applied metadynamics to dock small or sterically hindered ligands, predicting docking geometries and binding free energies.³¹ Recently, we have described a method which uses targeted steered MD in explicit solvent applied to dynamic molecular docking (DMD) of charged glycosaminoglycans into proteins.²²

In this work we use Replica Exchange Molecular Dynamics (REMD)³² in combination with a receptor-shaped piecewise potential, confining the ligand in the proximity of the receptor surface. REMD is commonly used to enhance sampling, especially if conformations are separated by relatively high energy barriers. It involves simulating multiple replicas of the same system at different temperatures and randomly exchanging the complete state of two replicas at regular intervals according to a probability that ensures the correctness of the ensemble sampling. So confined replica exchange MD (c-REMD) was applied to characterize the interaction of peptides with several protein–protein interaction domains. Our test set encompasses five docking cases including SH3, PDZ, GYF, and WW domains interacting with peptides characterized by

experimental dissociation constants spanning from μM to nM range. In each case, we correctly predicted the binding site and the experimental binding free energy (within a 1 kcal/mol error). In addition, it was possible to characterize the distinct poses adopted by the ligands in binding to the receptors, pointing out on the importance of considering the multiple binding modes in the determination of the overall binding free energy.³³

■ METHODOLOGY

Rationale for c-REMD and Its Characteristics. The adaptation of REMD to docking is built on the idea of implementing a method able to efficiently perform binding modes search (task generally assigned to docking) and, at the same time, to provide an ensemble of configurations useful for accurate binding affinity calculation (task generally assigned to MD simulations).

Such a method combines helpful aspects of both docking (e.g., reduced computational cost) and MD techniques (e.g., accurate sampling and consequently more reliable free energy evaluations), which provides obvious advantages. First, the binding modes search and the binding affinities calculation are carried out in one step instead of having to perform docking first and an MD approach afterward. In turn, it might be used as a midway alternative technique allowing a more effective interplay between these two techniques. Besides, such an intermediate method would be still able to use the solutions provided by molecular docking as starting guess for its own conformational sampling. Due to its higher complexity, such a midway method would not be able to replace docking in virtual screening. However, it might provide more exhaustive information on the structural disorder associated with given binding modes and increase the accuracy of the calculated binding affinities. Such a midway method would not be able to replace techniques such as all-atoms MD simulations in explicit solvent in terms of absolute accuracy, as it embraces certain approximations, but it might provide, within an affordable computational cost, better information than standard molecular docking and structures, which, being a higher level of accuracy then required, could be eventually exploited by proceeding with a more accurate MD calculations setup.

Consequently, the confined REMD method was tailored according to the following characteristics:

- It should use a reliable all-atoms force field (with point charges, Lennard-Jones parameters, bonded interactions).
- It should consider forces acting between ligand and receptor, as well as intrareceptor and intraligand interactions. The receptor secondary structure elements should remain invariable, whereas the side chains on the receptor surface would be fully flexible. The ligand would be fully flexible, and the formation of intramolecular hydrogen bonds should be considered.
- Solvent effects should be adequately treated. This means using at least a continuum solvent model, even if such an implementation must not set limits at the possibility to eventually consider the microsolvation effects due to few structuring of water eventually present at the binding site.
- It should be independent of previous knowledge on binding sites, like in the case of blind docking strategies.
- The sampling of the available conformational space should be efficient and reasonable in terms of computational cost.
- The solutions provided by c-REMD should follow a probability distribution, providing a thermodynamic ensemble

(i.e., canonical, NVT). Thus, binding free energies, free energy differences between bound states, and any other property should be accessible. In fact, on the contrary to most molecular docking approaches, c-REMD provides an ensemble of structures and not a best set of binding modes whose free energy has to be eventually evaluated individually. In principle, the entire surface of a receptor may be available for binding, although only one very favorable binding site is usually present. Nevertheless, at the binding site the ligand could adopt a huge plethora of conformations, although one or a few binding poses are generally preferred. However, it might happen that the number of secondary binding sites or poses, no matter how weak in binding, may be so abundant that their total contribution to the phenomenological (i.e., experimental) binding free energy should not be overseen. Thus, once an ensemble at equilibrium is obtained, it is possible to calculate the binding free energy through the number (probabilities) of bound or unbound configurations belonging to the ensemble. In the case of a unique dominant binding site, the phenomenological binding free energy is calculated considering the stability of the bound ligand in all accessible orientations and conformations, which might be both/either enthalpically and/or entropically favored. Instead, in the case of multiple binding sites, it may be possible to calculate the phenomenological binding free energy as a result of all contributions given by each binding site. In addition, it is also possible to calculate separately the binding free energy contribution of each binding site or binding pose.

Sampling Algorithm. In order to ensure the latter point, the search algorithms generally used in docking (i.e., systematic search, simulated annealing, genetic algorithm, fragment based algorithm)³⁴ must be replaced by a tool that might provide both an unbiased ensemble and an efficient sampling. Among MD methods reported in the literature, two of the most common are metadynamics and replica exchange molecular dynamics. Metadynamics³⁵ is aimed at reconstructing the multidimensional free energy landscape of complex systems, and it is based on a biased dynamics performed in the space defined by a few collective variables, which are assumed to provide an essential description of the system. The dynamics is driven by the free energy changes and is biased by a history-dependent potential constructed as a sum of gaussians centered along the trajectory of the collective variables. Accurate results can be obtained in a relatively short simulation time if the chosen collective variables are able to discriminate between the initial and final states and include all the modes relevant to the reaction. However, some variables often lack general applicability, or they are not able to distinguish between different basins. In molecular docking, variables defining the translation, rotation, and conformation of the ligand are typically used, but they lead to a metadynamics space that would be too large to be efficiently explored. However, the internal motions of the ligand might be neglected if the discarded degrees of freedom were fast enough to equilibrate during the simulation. This is the case of small or sterically hindered ligands. Instead, the choice of appropriate collective variables is harder in the case of ligands in which there is the necessity to include principal components of motions concerning slow conformational rearrangements. In order to overcome that problem, we chose the replica exchange (RE) method, due to its quick implementation and the possibility to perform a search stochastically driven by the diffusion over the potential energy

surface, without being forced to describe the system by means of a few collective variables that have to be chosen *a priori*.

c-REMD Procedure. In order to explore the conformational space of interest and rapidly identify the optimal binding modes, it is desirable that the ligand has an adequate mobility and that it principally resides close to the receptor surface (Figure 1). At lower temperatures the ligand spends most of

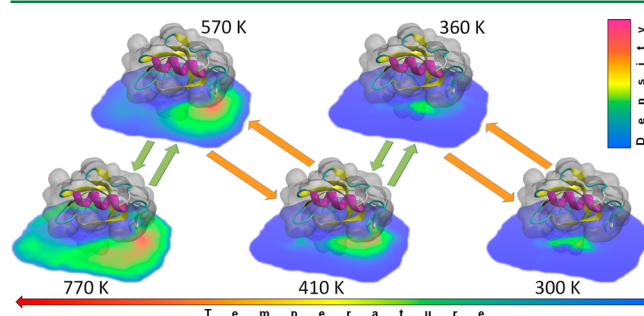


Figure 1. Texture mapped two-dimensional slices from the density distribution of the ligand backbone around PDZ domain at different temperatures. The molecular surface of the receptor is displayed in gray, whereas the slice is drawn in color scale as a plane passing through the receptor binding site. Only the unrestrained configurations with the ligand inside the confined volume were considered. In c-REMD, multiple replicas of the same ligand–receptor system are simulated at different temperatures, and randomly exchanged at regular intervals, alternating exchange attempts for all odd or even pairs (green and orange arrows) according to a probability that ensures the correctness of the ensemble sampling; a receptor-shaped piecewise potential restrains the ligand to be in proximity of the receptor surface, whereas inside the confined volume, no perturbations act on the ligand. At highest temperatures, the ligand rapidly spins around the receptor, efficiently sampling all accessible bound or unbound configurations. Decreasing the temperatures, the ligand progressively approaches the receptor surface in proximity of the binding site, until to definitely tie up at it at lowest temperature. Replicas at mid temperatures ensure to overcome energy barriers and allow an effective conversion between different ligand–receptor arrangements.

the time close to the receptor in a bound state, but its mobility is drastically reduced by the strong interaction with the receptor, and the sampling is poor. On the other hand, at higher temperatures the ligand has enough kinetic energy to overcome energy barriers, hence its mobility is adequate, but the ligand often moves away from the receptor, spending a considerable amount of time far from the receptor surface and leading to a consequent slow or poor sampling of the binding modes. A solution to this dilemma is to force the ligand to stay close to the surface of the receptor by adding a restraint. However, the application of restraints could introduce a bias in the ensemble distribution, and, in principle, it might also hinder the conformational changes of the ligand. Therefore, we considered a receptor-shaped piecewise potential that introduces a penalty only when the distance between the ligand and the receptor surface exceeds a threshold value (Figure 2). In this manner, it is possible to define a volume, shaped as the instantaneous solvent accessible surface (SAS) of the receptor, inside which the piecewise potential is null and no penalty forces act on the ligand, maintaining unbiased the conformational ensemble. Beyond the border of this volume, a restraint acts on the ligand confining its diffusion closely around the receptor. Because we are able to detect when the penalty potential is added on the basis of ligand position, it is possible

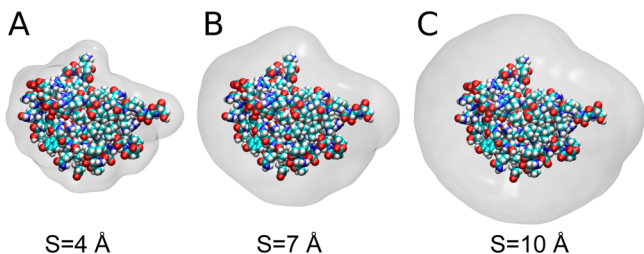


Figure 2. Boundaries of the region where the receptor-shaped piecewise potential is null as a function of distance parameter S . During c-REMD the ligand is forced to reside inside the gray surface where no penalty potential is applied. The boundaries are built so to be similar to solvent accessible surface (SAS) of the receptor and instantaneously updated during the simulation upon receptor rearrangements.

to collect only the configurations where the penalty potential is null, thus providing an unbiased ensemble. The threshold value of the distance between the ligand and the receptor surface has to be chosen accurately. Large values provide a poor sampling of the bound configurations of interest (i.e., binding modes), and small values reduce too much of the space available for the ligand to perform structural rearrangements. The optimum value should be chosen such that at the border of the confined space the perturbation applied by the receptor on the ligand conformation is negligible. Indeed, the conformations adopted by the ligand in proximity of the border, inside the confined volume, would be representative of all conformations that the ligand adopts in the absence of restraints at infinitive dilution. In this manner the thermodynamic contribution due to the conformations that the ligand would adopt in the absence of a restraint outside the confined volume might be simply considered in terms of change in translational entropy.

Receptor Surface Detection. In order to identify the atoms lining the protein surface and thus the residues to be maintained flexible, the circular variance CV was used to measure the grade of “insideness” of a given residue with respect to a set of atoms. The concept of circular variance and its applications in surface detection, domain separation, and pocket definition can be deepened elsewhere.³⁶ Briefly, given a position \mathbf{R}_0 and a set of points $\{\mathbf{r}_i\}$, the circular variance CV for a sample of vectors drawn from \mathbf{R}_0 to each point \mathbf{r}_i belonging to $\{\mathbf{r}_i\}$ can be calculated as

$$CV = 1 - \frac{|\sum_{i=1}^N (\mathbf{R}_0 - \mathbf{r}_i)/\|\mathbf{R}_0 - \mathbf{r}_i\||}{N}$$

where N is the number of points in $\{\mathbf{r}_i\}$. When \mathbf{R}_0 is infinitely far from $\{\mathbf{r}_i\}$, all vectors drawn are parallel, thus the vector and scalar sums coincide, resulting in $CV = 0$; when \mathbf{R}_0 is in the “middle” of $\{\mathbf{r}_i\}$, the vector sums tend to zero, resulting in $CV = 1$. Therefore, CV can provide a quick and reasonable (however approximate) measure of how deep inside or how far outside the cloud formed by $\{\mathbf{r}_i\}$, the point \mathbf{R}_0 is. The choice of atoms positions to be included in the set $\{\mathbf{r}_i\}$ provides an option for further refinements. The simplest tool for such selection is to introduce a limit for the distance between the query point \mathbf{R}_0 and the points included in $\{\mathbf{r}_i\}$. This not only offers a reduction of the computational effort but also allows for the control of “smoothing” the transition observed for CV at the limit of the sample of points $\{\mathbf{r}_i\}$. A 9 Å cutoff was used in all calculations of atomic circular variance, and all atoms in a position with

circular variance lower than 0.7 were considered to outline the protein surface.

Once the residues belonging to the protein surface were detected, their side chains were left free to move during the simulation, whereas the rest of the protein was kept fixed by means of holonomic constraints. Because the protein is unable to undergo conformational changes at a level of secondary/ternary structure during the simulation, the set of external residues is substantially invariant. However, if conformational changes in the protein backbone were allowed, the list of surface residues might be quickly updated. Neglecting the conformational changes at the level of the receptor backbone was taken into account especially in consideration of the choice of the receptors to be used in our tests. In fact, neglecting the displacements of the receptor backbone is a limitation that might be tolerable if we consider that, during the unconstrained simulation (data not shown), the test receptors actually underwent poor backbone rearrangements, and their root-mean-square fluctuations were limited and with unimodal distributions. The motion of the receptor backbone will be instead addressed and introduced in future work (e.g., using essential dynamics sampling, which can introduce some grade of flexibility). The current work’s focus resides in assessing the convenience and the correctness of the methodology on a set of relatively complex systems with given characteristics (*vide infra*).

Receptor-Shaped Piecewise Potential Definition. The set of external residues can be used to define a receptor-shaped piecewise potential, which is dependent on the distance between the receptor surface and the ligand. Because the contours of a so-built potential would depend solely on the instantaneous positions of the atoms belonging to protein surface, the borders of the potential are updated at each step as a consequence of the motion of the external residues. The potential depends essentially on a single parameter S , which has distance dimensions. When S is lower than a given value S_1 , the potential is null and no forces act. When S has values between S_1 and S_2 , the potential is quadratic as a function of the parameter S , whereas beyond S_2 the potential becomes linear as a function of the parameter S . The forces are always orthogonal to the isosurface formed by the points with a constant value of S . Such isosurfaces have the quality to be similar to the SAS of the receptor (see Figure 2). Given a position \mathbf{P}_0 and a set of coordinates $\{\mathbf{p}_i\}$ the value S can be calculated as

$$S = \left(\sum_{i=1}^N \|\mathbf{P}_0 - \mathbf{p}_i\|^{-2n} \right)^{-1/2n}$$

where n is an integer. For $n \rightarrow \infty$, S coincides with the smallest distance between \mathbf{P}_0 and the set $\{\mathbf{p}_i\}$. In this particular case with $n = 3$, it provides a smooth and efficient approximation of the $\min(\|\mathbf{P}_0 - \mathbf{p}_1\|, \|\mathbf{P}_0 - \mathbf{p}_N\|)$ function. Because the set of coordinates $\{\mathbf{p}_i\}$ represents the positions of atoms belonging to the receptor surface, the receptor-shaped piecewise potential can be defined using only the parameter S . The set of atoms used to define the potential might be, for computational efficiency reasons, also a subset of atoms belonging to the receptor surface. Of all atoms detected by means of the circular variance method previously described, only the subset of heavy atoms was initially considered. Because neighboring covalently bonded atoms occupy similar positions in space, the coordinates of all heavy atoms represent a set of redundant information for describing the receptor shape and the

boundaries of the receptor surface. In order to reduce the computational cost, the number of atomic coordinates was decreased by considering only a specific subset of heavy atoms for each residue. The aim was to represent the position of a group of 3–4 heavy atoms by means of a single central atom, resulting in a 4-to-1 mapping. The potential was applied to the ligand onto a single atom for each residue (i.e., all C_α atoms of a peptide or all anomeric oxygen atoms of an oligosaccharide).

■ TEST MODELS

The systems used to test c-REMD were chosen in order to reach a compromise between system complexity and computational effort. The following criteria were used for selection: the ligand should contain no more than about ten residues, the receptor should not exceed 100 residues, the experimental structure of the ligand–receptor complex at high resolution should be available, the corresponding experimental dissociation constants should be known, the receptor should not undergo relevant conformational changes at the backbone throughout the ligand binding, and experimentally there should not be concurrent or coupled mechanisms with the ligand–receptor binding (i.e., no dimerization or superstructural assembling). Accordingly, we chose five test cases among several protein–protein interaction domains responsible for the molecular recognition of specific peptide sequences (Figure 3):

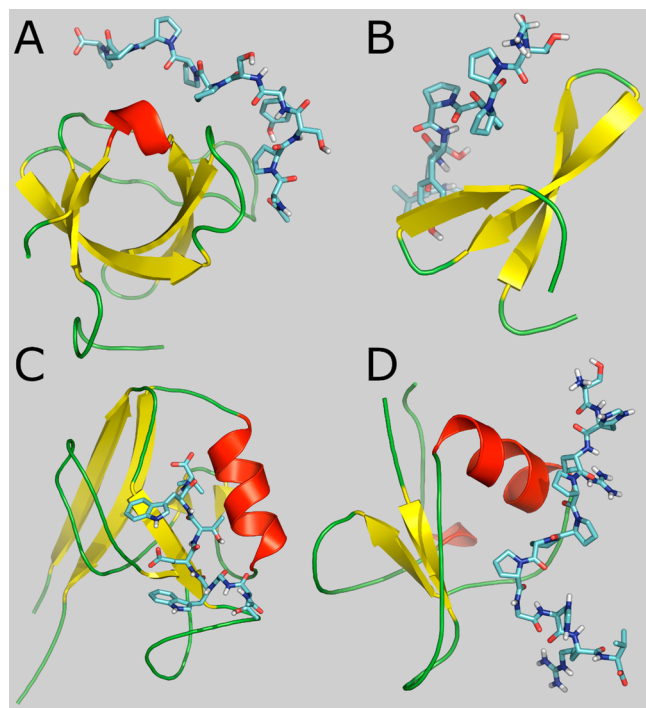


Figure 3. NMR structures of the ligand–receptor systems used as templates for testing c-REMD. Receptors are shown in cartoon, whereas ligands are shown in sticks. A) the R21A mutant of the α -spectrin SH3 domain in complex with the decapeptide p41 APSYSPPPPP (PDB ID 2jma). B) the L30K mutant of the WW domain belonging to the Yes kinase-associated protein 65 (YAP65) in complex with the decapeptide GTPPPPPYTVG (PDB ID 1jmq). C) the PDZ domain of Erbin, a member of the LAP (leucine-rich repeat and PDZ-containing) protein family, in complex with the peptide AcTGWETWV (PDB ID 1n7t). D) the GYF domain of CD2BP2 protein adaptor in complex with the SHRPPPGHR peptide (PDB ID 1l2z).

the R21A mutant of the α -spectrin SH3 domain in complex with the decapeptide APSYSPPPPP p41 (PDB ID 2jma, SH3),³⁷ the wild type form and the L30K mutant of the WW domain belonging to the Yes kinase-associated protein 65 (YAP65) in complex with the decapeptide GTPPPPPYTVG (PDB ID 1jmq, WW_{wt} and WW_m),³⁸ the PDZ domain of Erbin, a member of the LAP (leucine-rich repeat and PDZ-containing) protein family, in complex with the peptide AcTGWETWV (PDB ID 1n7t, PDZ)³⁹ and, finally, the GYF domain of the CD2BP2 protein adaptor in complex with the SHRPPPGHR peptide (PDB ID 1l2z, GYF).⁴⁰ All were experimental structures obtained in solution by NMR. The capping of each peptide terminus was set according to the experimental conditions previously used to measure the dissociation constants.

Src-homology region-3 (SH3) domains are small proteins modules mediating transient protein–protein interactions relative to a large number of cellular processes.^{41–43} SH3 domains recognize proline-rich sequences through a highly conserved mode of interaction, with binding affinities ranging between 5 μ M and 100 μ M.^{44,45} Its basic fold contains five antiparallel β -strand packed to form two perpendicular β -sheets; the binding site consists of a hydrophobic patch that contains a cluster of conserved aromatic residues and is surrounded by two charged and variable loops. The WW domains form a family of protein modules, composed by ~38 amino acids, that folds into a three-stranded β -sheet, with high content of hydrophobic, aromatic, and proline residues and two highly conserved tryptophan residues within the consensus sequence.⁴⁶ Like other intracellular protein modules, the WW domain is present in a variety of cytoskeletal and signal-transducing proteins, such as YAP65.^{46–48} They bind proline-rich peptides, as do SH3 domains, and WW and SH3 domains may compete for binding to the same sequence motifs.⁴⁹ The PDZ domain, so-called because it was first recognized in the protein postsynaptic density-95, discs large, and zonula occludens 1,^{50–52} is a common component composed of ~90 residues that adopts a common fold consisting of a β -barrel capped by α -helices and ligands bind adopting β -strand or extended conformations.⁵³ The glycine-tyrosine-phenylalanine (GYF) domain was first reported in the CD2 binding protein (CD2BP2) as a domain capable of binding to a proline-rich peptide sequence in the CD2 tail region. Despite functioning as a proline-rich peptide binding domain, the GYF fold is structurally unrelated to the SH3 or WW domains, forming a unique bulge-helix-bulge motif, in which a single α -helix is tilted away from a twisted antiparallel β -sheet.

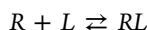
■ SIMULATION METHODS

c-REMD calculations were performed using the Gromacs 4.5.4 software package⁵⁴ and AMBER force field.⁵⁵ Each system was placed in a cubic box, and periodic boundary conditions were applied for computational efficiency reasons; the dimensions of the box (with edge of 10–11 nm) were set to deny the interaction between the system and its periodic images and to avoid the inversion of the force applied by the receptor-shaped piecewise potential (cause of the use of the periodicity in distance calculation). The receptor was located at the center of the box, and holonomic constraints were applied to maintain fixed the coordinates of the atoms belonging to the receptor interior, whereas the receptor atoms near the surface and the ligand were maintained unrestrained. Covalent bonds with hydrogen atoms were constrained to their equilibrium values by

the LINCS algorithm,⁵⁶ enabling a 2 fs time step. Temperatures were maintained constant using a stochastic thermostat⁵⁷ with a temperature coupling of 10 fs. The solvent was treated implicitly using the Generalized Born formalism augmented with a solvent accessible surface area term (GBSA) and the Still method⁵⁸ for calculating Born radii. Such an implementation permits to drastically scale down the number of degrees of freedom of the system and, therefore, the number of replicas, and it allows for speeding up the conformational sampling reducing or omitting the medium viscosity. At the same time, in the absence of structuring water molecules or of relevant microsolvation effects, such an approximation is in line with some other methods (e.g., docking or MM/PBSA) but takes advantages of its augmented conformational sampling. A cutoff of 1.6 nm was used for Coulomb interactions, whereas a pair list cutoff of 1 nm was used for van der Waals interactions. Neighbor lists were updated every fifth step. REMD simulations were performed in a range of temperature spanning from 300 to 900 K, and the temperature distributions were generated⁵⁹ in order to obtain an exchange probability of 0.4 (Figure S1). A total of 24, 24, 30, 30, and 32 replicas were used for WW_w, WW_m, SH3, GYF, and PDZ, respectively. Exchange between replicas was attempted every 5 ps, leading to an exchange rate of about 24/ns. The exchange time and probability were chosen to have an adequate frequency of exchanges between a number of replicas, such that to efficiently explore the different positions of the ligand on the receptor surface. The highest temperature was chosen to have a high search rate, avoiding the system to be trapped in local minima and rapidly diffuse over the receptor surface. In order to ensure numerical stability, the hydrogen atoms were replaced by deuterium. It is worth noting that the latter implementation affects the kinetics but not the thermodynamics of the system. The initial velocities for each replica were taken randomly from Maxwellian distributions. The receptor-shaped piecewise potential was implemented exploiting the distance restraints feature included in Gromacs; a force constant of 400 kJ/mol nm⁻² was applied between each C_α atom of the ligand and the atoms used for defining the receptor surface. The receptor-shaped potential was null below a specified lower bound, quadratic between the lower and the higher bound, and linear beyond the higher bound. Distances of 1 and 1.2 nm were used for the lower and higher bound, respectively, for all systems, at the exception of SH3 and PDZ where 0.9/1.1 nm distances were used. Such a setup ensured a free volume with unbiased potential around the receptor with a thickness of 8–10 Å (Figure S2) and a fraction of distance violations for the piecewise potential less than 0.2% at lower temperatures. For each system, the initial coordinates of the receptor were taken from the structure deposited in the protein databank (PDB), whereas the ligand, in unbound conformation, was placed in a position angularly unrelated and far from the expected binding site (Figure S3). For each system we performed a productive simulation of 120 ns, neglecting the first 10 ns in following analyses.

BINDING FREE ENERGY CALCULATIONS

Receptor–ligand interactions involve physical contact between the ligand and the receptor. These contacts are specific and result in an attractive force. The receptor–ligand interactions are, in general, dependent on the concentration of the ligand, receptor, and salts in the solution. The expression



represents a chemical interaction. Here, R is the receptor, L is the ligand, and RL is the receptor–ligand complex.

The binding and dissociation equilibrium constants can be defined as

$$K_b = \frac{[RL]}{[R][L]} \quad K_d = \frac{1}{K_b} = \frac{[R][L]}{[RL]}$$

Let p_{bon} and p_{unb} be the fraction of the ligand respectively bound or unbound to the receptor. Because two distinct regions of the configurational space can be distinguished without ambiguity, i.e. the binding sites and the bulk unbound regions, it follows that $[L] = p_{unb}[L]_{tot}$ and $[RL] = p_{bon}[L]_{tot}$ where $[L]_{tot}$ is the total concentration of the ligand in the system. By normalization, being either zero or one ligand L bound to the receptor R, $p_{bon} + p_{unb} = 1$. It follows that the binding constant can be expressed as

$$K_b = \frac{p_{bon}[L]_{tot}}{[R]p_{unb}[L]_{tot}} = \frac{1}{[R]} \frac{p_{bon}}{p_{unb}} = \frac{V}{V_0} P$$

where P is a partition coefficient of the ligand between its bound and unperturbed unbound state, and the concentration of the receptor in mol/liter is expressed as the ratio between V , the confined volume of the simulation system where the receptor-shaped potential does not act, and V_0 the volume corresponding to the chosen standard state: for example, 1660 Å³ on an atomic basis for a one molar standard state.

A fundamental thermodynamic equation relates the free energy change associated with a binding reaction when all reactants and products are present at 1 molar concentration with changes in enthalpy and entropy:

$$\Delta G = \Delta H - T\Delta S$$

The binding constant at equilibrium can be related to the free energy change as

$$\Delta G = -RT \ln K_b = -RT \ln P - RT \frac{V}{V_0}$$

or arranging

$$\ln P = -\frac{\Delta H}{RT} + \frac{\Delta S + R \ln V_0/V}{R} = \frac{a}{T} + b \quad (1)$$

Because each bound configuration that we can obtain from MD simulations might differ by the position or the orientation of the ligand, or by any other structural feature, we might desire to cluster the bound configurations into substates according to some given criteria. At that point, it would be useful to calculate the contribution, given by each substate or binding mode, to the overall binding. Defining f_i the fraction of bound configurations corresponding to a generic binding mode i , as

$$f_i = \frac{p_{bon,i}}{p_{bon}} = \frac{p_{bon,i}}{\sum p_{bon,i}} \quad \text{with} \quad \sum f_i = 1$$

it follows that

$$\Delta G_{bin,i} = \Delta G_{bin} - RT \ln f_i \quad K_{d,i} = \frac{K_d}{f_i}$$

where $\Delta G_{bin,i}$ and $K_{d,i}$ are respectively the binding free energy and the dissociation constant owing to the generic binding mode i .

RESULTS

For each of the test systems studied, REMD simulations provided us a canonical ensemble of the ligand–receptor system at each specific temperature considered. It means that we can follow the evolution of either thermodynamic or structural properties for each replica; as illustrations of this capability, we report respectively in Figures S4–S7 the time series of temperatures, of the replica indices, of the deviation from the experimental binding mode, and of the minimum distance between ligand and receptor, determined for the PDZ test case. In addition, at each replica temperature, it is possible to calculate P as the ratio of the times in which the ligand is bound to receptor and the times in which the ligand is unbound. We defined the bound and unbound states according to a cutoff criterion, considering the ligand bound if its shortest distance from the receptor is less than a given value. Obviously the value of P depends on the cutoff value. If the cutoff were 0, the ligand would be always in an unbound state, whereas if the cutoff were infinite, the ligand would be always in a bound state. Consequently, the first derivative of the binding free energy with respect to the cutoff, averaged between 3.2 and 3.8 Å, falls in the range of -30 and -37 kJ/mol Å for all test cases with the exception of the PDZ domain, whose value is -46 kJ/mol Å (Figure S8). Because the choice of a cutoff may be arbitrary, and considering its influence on the measured binding affinity, it is fundamental that, once defined the bound and unbound state, this definition must be applied for all systems studied. Therefore, the cutoff was set to 3.5 Å. Interestingly, such a value, which was initially chosen because it is commonly used as a limit for defining the formation of hydrogen bonds or contacts between molecules, falls in the range of cutoffs that best interpolates the binding free energies with the experimental data. Plotting the natural logarithm of the partition coefficient P versus the reciprocal temperature and considering ΔH and ΔS virtually constant in a range of temperatures, it would be possible to extrapolate the partition coefficient (and therefore the binding free energy) at 300 K and to estimate ΔH and ΔS from the slope and intercept of the straight line so obtained (see eq 1). In Figure 4 we report the Van't Hoff plot for SH3, PDZ, WW_{wt}, WW_m, and GYF in a range of temperature between 300 and 450 K. Note that the high linear correlation of the points allows us to apply eq 1 and obtain ΔH and ΔS . It also means that, due to the particular setup of the simulations, the difference of specific heat capacity ($\Delta\Delta c_p$) between bound and unbound ligand/receptor is virtually negligible. In Table 1, we report for each system the data used for the calculation of the thermodynamic quantities. The volume V is the volume that includes all points where the receptor-shaped piecewise potential is null and was calculated by means of a grid method; the grid mesh resolution was progressively augmented until a specified threshold.

In Figure 5 the values of binding free energy calculated by means of c-REMD are plotted as a function of the experimental binding free energies, derived from the dissociation constants measured at 298 K by fluorescence or calorimetric titration experiments for SH3 ($K_d = 55 \mu\text{M}$),³⁷ PDZ ($K_d = 0.15 \mu\text{M}$),³⁹ WW_{wt} ($K_d = 52 \mu\text{M}$),⁶⁰ WW_m ($K_d = 40 \mu\text{M}$),⁶⁰ and GYF ($K_d = 206 \mu\text{M}$).⁴⁰ The agreement with the experimental data is very high in the whole range of dissociation constants considered. The error, which is within ± 1 kcal/mol for all systems, principally depends on the approximations introduced (rigid backbone, implicit solvation, etc.). However, it is reasonable

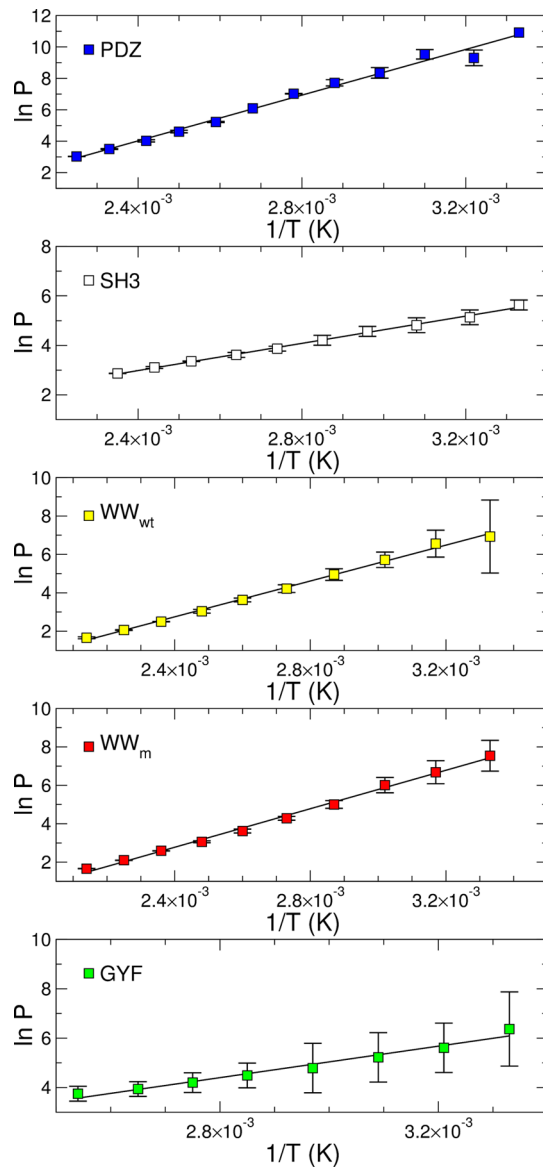


Figure 4. Van't Hoff plot for the R21A mutant of the α -spectrin SH3 domain in complex with the decapeptide p41 APSYSPPPPP (SH3, white squares), the PDZ domain of Erbin in complex with the peptide AcTGWETWV (PDZ, blue squares), the L30K mutant (WW_m, red squares) and wild type form (WW_{wt}, green squares) of the WW domain belonging to the Yes kinase-associated protein 65 (YAP65) in complex with the decapeptide GTPPPPYTVG, the GYF domain of CD2BP2 protein adaptor in complex with the SHRPPPGH peptide (GYF, yellow squares) in a range of temperature between 300 and 450 K. Error bars were obtained comparing the two halves of the productive simulation.

that the error should depend also on the system considered and that, if all others conditions are fixed, it is almost constant for a given system. Hence, we could compare the results of two very similar systems (i.e., mutants), detecting differences in binding affinity, even significantly smaller than the error. This is the case of WW domain, where the mutation L30K is predicted to slightly affect the stability of the complex with the peptide GTPPPPYTVG, in agreement with the experiments, and increase the binding free energy by 0.8 kJ/mol.^{38,60} The calculated binding free energies and the corresponding dissociation constants are reported in Table 2, where they are

Table 1. Thermodynamic Parameters as Obtained by Linear Least Squares Fitting in van't Hoff plots^a

system	<i>a</i> (K)	<i>b</i>	<i>V</i> (Å ³)	<i>V</i> ₀ / <i>V</i>	Δ <i>H</i> (kJ/mol)	Δ <i>S</i> (J/mol K)	Δ <i>G</i> (kJ/mol)	<i>K</i> _d (μM)
PDZ	7273	-13.432	79937	0.021	-60.4	-79.4	-36.8	0.36
SH3	2756	-3.630	59680	0.028	-22.9	-0.397	-22.8	101
WW _{wt}	4664	-8.440	49340	0.034	-38.8	-41.9	-26.3	25
WW _m	5010	-9.250	49340	0.034	-41.6	-48.7	-27.1	18
GYF	3104	-4.526	74501	0.022	-25.8	-6.00	-24.0	62

^aSH3: Spc SH3 R21A/AcAPSYSPPPPP; PDZ: Erbin PDZ/AcTGWETWV; WW_{wt}: YAP65 WW/GTPPPYYTVG; WW_m: YAP65 WW L30K/GTPPPYYTVG; GYF: CD2BP2 GYF/SRPPPGHHRV.

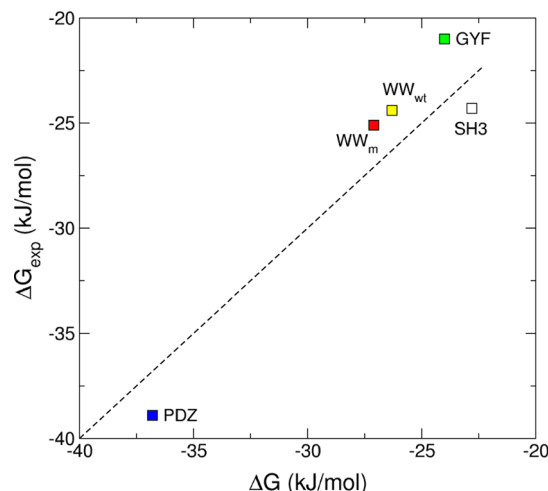


Figure 5. Values of binding free energy calculated by means of c-REMD (Δ*G*) plotted as a function of the corresponding experimental binding free energies (Δ*G*_{exp}), derived from the dissociation constants measured at 298 K by fluorescence or calorimetric titration experiments.

compared with the corresponding experimental data. The numbers in parentheses represent the contribution given to the binding free energy by the same portion of the receptor surface involved in binding in the resolved structures (expected binding site). Calculating these contributions, no distinctions were made between the different ligand orientations and conformations; although involving the same receptor binding site, the configurations adopted by the ligand might be significantly different from the binding mode experimentally observed by crystallography or high resolution NMR. Therefore, the ligands mainly occupy the same receptor binding site although they can adopt several binding modes. Thus, the AcAPSYSPPPPP

peptide binds the Spc SH3 domain to the cleft in between the RT loop and the n-Src loop, GTPPPYYTVG has often contacts with at least one of the key residues Tyr28, Leu30, and His32 lining the binding cleft of WW domain, and the AcTGWETWV peptide binds the Erbin PDZ domain in the region corresponding to the β₂-β₃ strands (see Figure 7, upper panels). For CD2BP2 GYF domain, the crystallographic structure of the binding mode is not available. Experimental NMR titrations with peptides containing one or two consensus sequences, respectively, suggest that probably there are multiple potential binding sites on the GYF receptor surface. We observe that the ligand patches the GYF domain in the cleft delimited by the β₁-β₂ and the β₃-β₄ loop, whereas the region occupied by the conserved residues G32, Y33, and F34 is only the second most populated binding site.

In order to assess the capability of the methodology to take adequately into account the determinants of molecular recognition between ligand and receptor, we used a negative control by calculating the binding affinity of a nonbinding peptide for its expected binding site. As a test case, we considered the SPPPPATV peptide, which lacks the PPPY consensus sequence and does not bind the WW domain.⁶⁰ As expected, for such a peptide the calculated binding affinity drops considerably, down to 10.5 kJ/mol with a *K*_d of 15 mM.

In all test sets, constraining the receptor side chains to the PDB coordinates, the experimentally expected binding mode turned out to be the most stable and the deviations from it were very small. In addition, it contributed almost completely to the binding affinity, even if, in that case, this one became 5–8-fold smaller than that experimentally measured in solution. This fact suggests that the rearrangement of the receptor surface in solution might bring the ligand to adopt a plethora of different binding modes that taken together give the total binding affinity experimentally observed. We clustered the configurations of the ligands in the respective binding site according to their root-

Table 2. Theoretical and Experimental (exp) Thermodynamic Properties Associated with the Binding of the Ligand to the Receptor^a

receptor	ligand	Δ <i>H</i> (kJ/mol)	TΔ <i>S</i> (kJ/mol)	Δ <i>G</i> (kJ/mol)	<i>K</i> _d (μM)	Δ <i>G</i> (exp) (kJ/mol)	<i>K</i> _d (exp) (μM)
Erbin PDZ	AcTGWETWV	-60.4	-23.7	-36.8 (-36.8)	0.36 (0.36)	-38.9	0.15
Spc SH3 R21A	AcAPSYSPPPPP	-22.9	-0.1	-22.8 (-22.7)	101 (111)	-24.3	55
YAP65 WW	GTPPPYYTVG	-38.8	-12.5	-26.3 (-23.6)	25 (77)	-24.4	52
YAP65 WW L30K	GTPPPYYTVG	-41.6	-14.5	-27.1 (-23.5)	18 (80)	-25.1	40
CD2BP2 GYF	SRPPPGHHRV	-25.8	-1.8	-24.0 (NA)	62 (NA)	-21.0	206

^aIn parentheses the contribution given by the expected binding site.

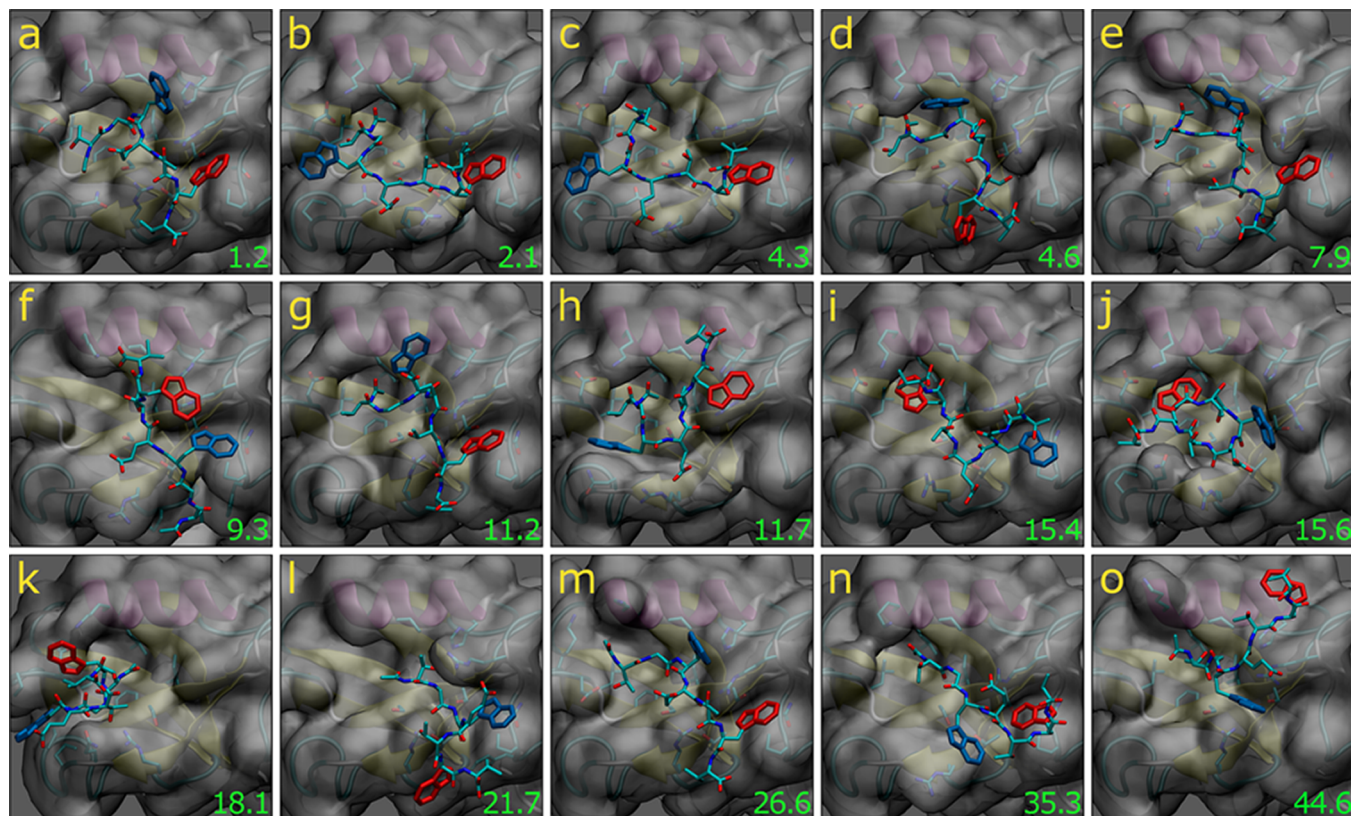


Figure 6. Representative structures of the 15 most populated clusters as obtained using the linkage method with a cutoff of 0.15 nm on the collected configurations of $\text{AcTGW}^{-4}\text{ETW}^{-1}\text{V}$ peptide bound to the PDZ domain (a-o). The corresponding dissociation constants in μM are reported in light green. The peptide is depicted in sticks, with the tryptophan residues highlighted: W^{-4} in blue, W^{-1} in red.

mean-square deviation (RMSD), using a cutoff of 1.5 \AA . In Figure 6 the representative configurations of the first 15 most populated clusters are reported for the AcTGWETWV peptide bound to Erbin PDZ domain. The first 15 clusters of the 468 found contain respectively 4916, 2980, 1423, 1315, 770, 656, 547, 521, 398, 391, 337, 282, 230, 173, and 137 structures, including together $\sim 90\%$ of the 16975 structures used for the RMSD matrix calculation. The binding modes depicted in Figure 6 have respectively binding free energies of -33.7 , -32.5 , -30.6 , -30.4 , -29.1 , -28.7 , -28.2 , -28.1 , -27.4 , -27.4 , -27.0 , -26.6 , -26.1 , -25.4 , and -24.8 kJ/mol which correspond to dissociation constants ranging from 1.2 to $44.6 \mu\text{M}$. Obviously such results depend on the method and the parameters used during the configuration clustering; using a cutoff of 1 \AA , for example, 3636 clusters were found, and the binding free energy of the most populated binding mode decreases to -32.4 kJ/mol . However, it is worth further remarking the importance of considering multiple binding modes in order to correctly calculate the binding free energy.³³ In fact the first binding mode has a binding free energy significantly smaller than the experimental one, 5.2 kJ/mol , a difference which decreases to 2.4 kJ/mol , considering for example the 15 clusters together.

Similarly, the cluster analysis of AcAPSYSPPPPP peptide in Spc SH3 binding site found 2077 clusters using a cutoff of 1.5 \AA , with the binding free energy of the most populated binding mode of -16.4 kJ/mol (see Figure S9). The dissociation constants of the most populated binding modes depicted in Figure S9 range from 1.5 to 7.1 mM and together cover only 55% of the total binding affinity. That suggests a more

pronounced variability with whom the peptide can arrange in the SH3 binding site, with respect to that previously observed in the case of PDZ domain. The cluster analyses of the GTPPPPYTVG peptide bound to the WW domain and its L30K mutant found 393 and 294 clusters, respectively. The most populated binding modes are depicted for wild type (wt, Figure S10) and mutant (Figure S11), and their dissociations constants range from hundreds of μM to tens of mM. Taken together the 15 best binding modes contribute to $\sim 95\%$ of the total dissociation constant calculated for the expected binding site of the WW domain, both for wt and the L30K mutant. However, the dissociation constants of the first two binding modes in wt WW cover the 83% of the total, whereas in the mutant they cover only 45% . This fact suggests that the L30K mutation increased the structural disorder of the peptide in correspondence to the WW domain binding site, allowing other arrangements to be more accessible and populated, with the final effect to slightly augment the whole binding affinity. Unfortunately, for the GYF domain it is not possible to assign an unambiguous and delimited binding site, as experimental mutational and structural analyses have shown a very extended, conserved signature $\text{W-X-Y-X}_{6-11}\text{-GPF-X}_4\text{-M-X}_2\text{-W-X}_3\text{-GYF}$ to be the site of interaction with proline-rich peptides.⁶¹ Our cluster analyses have shown that the peptide binds GYF in different regions, involving one at a time, with different groups of residues belonging to the consensus sequence. Considering only the region at the center of all residues of the consensus sequence, we obtain a scattered group of configurations that contribute to the total binding free energy for -17.5 kJ/mol ($K_d \sim 900 \mu\text{M}$). Clustering such configurations further, using a

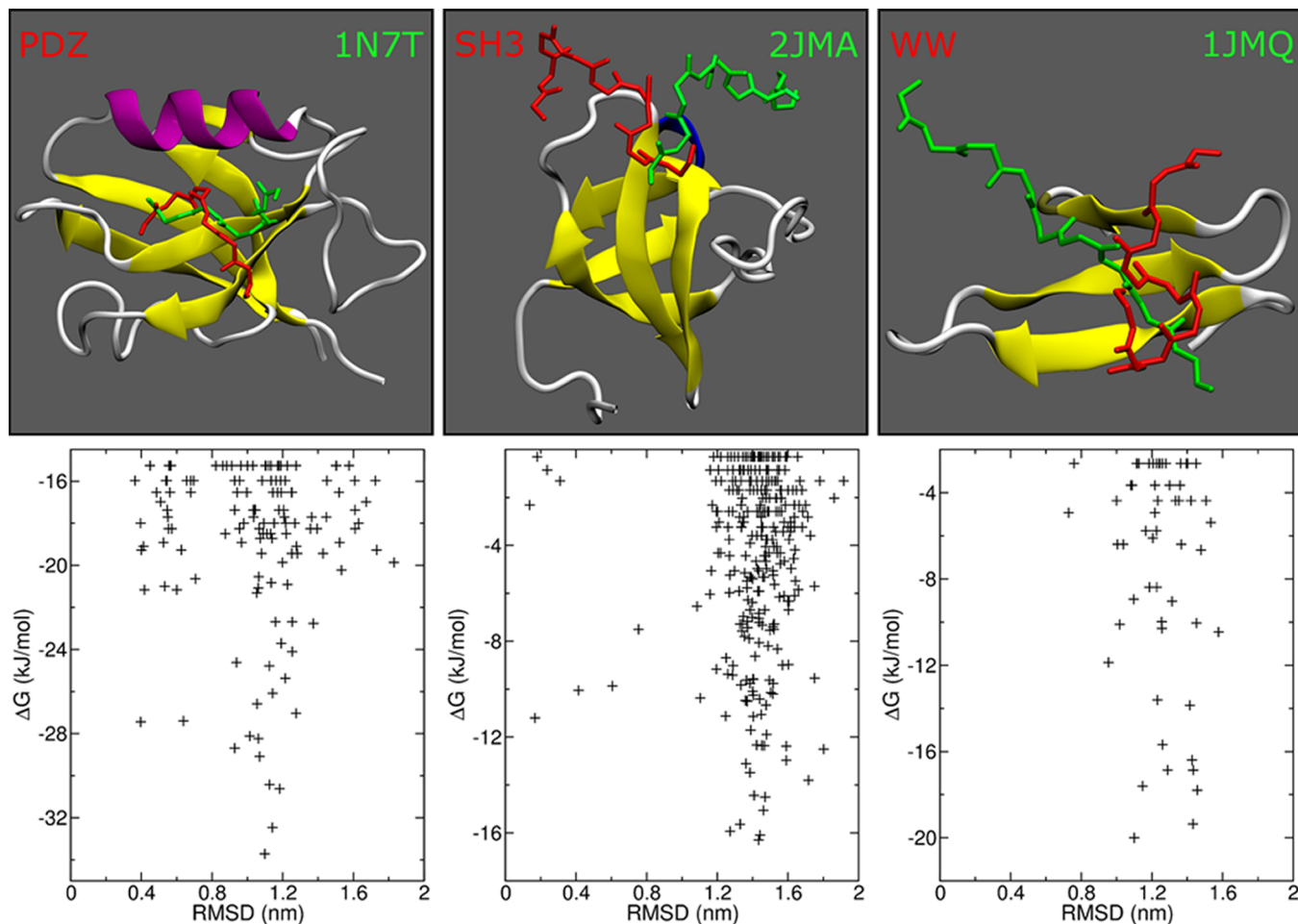


Figure 7. Upper panels: comparison between the most stable binding mode, obtained by c-REMD, and the experimental binding mode, obtained by NMR refinement; the computed (red) and the experimental (green) ligand backbones were superimposed after the least-squares fitting of the receptor backbones. Bottom panels: binding free energy of the most stable clusters obtained by c-REMD is plotted vs backbone root-mean-square deviation (RMSD) between the computed and the experimental binding mode.

RMSD cutoff of 1.5 Å, 293 clusters were found. Among them, the 15 most populated clusters correspond to the binding modes depicted in Figure S12, with dissociation constants ranging from 4 to 100 mM.

In Figure 7, we compare the most stable binding mode, obtained for three domains (PDZ, SH3, WW_m), with the respective docked structures experimentally obtained by NMR refinement (1N7T, 2JMA, 1JMQ). In the upper panels, the computed (red) and the experimental (green) conformations of the ligand backbone are superimposed after the least-squares fitting of the receptor backbones. In all three cases, the computed ligand conformation resides in the expected binding site, and it completely or partially overlaps the experimental conformation. In the bottom panels, the calculated binding affinity for the expected binding site is plotted as a function of the RMSD, for each of the calculated binding modes. Interestingly, in the case of the PDZ and SH3 domain, some binding modes are similar to the experimental one (RMSD < 4 Å), although their calculated binding affinity is lower than that obtained for the most stable binding mode. Instead, in the case of the WW domain, the simulation does not sample the extended conformation proposed by the NMR refinement, but bent or other conformations, which augment the contact with the receptor, are preferred.

In Table 2 we report also the contribution given by the enthalpy or entropy to the ligand binding as obtained by the calculations. Because the use of a continuous model for the treatment of the solvent does not permit considering the contribution to enthalpy and entropy given by the rearrangement of the solvent upon ligand binding, the calculated data cannot be directly compared with the experimental ones. For example in the case of SH3 the calorimetric experiments provide a binding enthalpy of -58.7 kJ/mol and a $T\Delta S$ term of -34.4 kJ/mol,³⁷ which are to be compared with -22.9 kJ/mol and -0.1 kJ/mol (provided by the calculations), respectively. It is worth noting that despite the marked differences observed in the calculated binding enthalpy and entropy with respect to the experimental data, the calculated binding free energy is surprisingly in agreement with the experiments. Such a contradiction might be explained on one hand by the fact that upon ligand binding the rearrangement of the solvent could provide more stable but also more ordered structures, and therefore a change in enthalpy might be in part compensated by a corresponding change in entropy. On the other hand, such a result shows that the force field parameters in combination with implicit solvent models are in some measure adjusted to include small net contribution due to the solvent rearrangement, allowing the correct prediction of the binding free energies.

Although conventional molecular docking methods provide low RMSD values for the docked poses of the ligands, they are generally unreliable for prediction of binding affinity. Among our test cases, the TGWETWV peptide and its receptor Erbin PDZ is a system commonly reported in the literature and being used for flexible molecular docking calculations to explore the binding selectivity of such a class of domains.^{62,63} Gerek and Ozkan⁶² performed docking using the ROSETTALIGAND⁶⁴ protocol, included in the ROSETTA package, in combination with DrugScore,⁶⁵ a knowledge-based scoring function that employs statistically derived pair potentials. ROSETTALIGAND, which is specifically developed for docking ligands into protein binding sites, reproduced the experimental binding mode of TGWETWV peptide on the native structure of PDZ domain (PDB ID 1n7t), with a RMSD of only 0.83 Å, but with an expected binding affinity of -69 kJ/mol, whereas DrugScore predicted for the same binding mode a binding free energy of -972 kJ/mol. Niv and Weinstein,⁶³ using a flexible docking scheme (termed PDZ-DocScheme), based on simulated annealing molecular dynamics and rotamer optimization, found a best binding pose with a RMSD of 1.7 Å and a score of ~220 kJ/mol.

CONCLUSIONS

c-REMD has been implemented combining replica exchange molecular dynamics with a receptor-shaped piecewise potential, which confines the ligand in the proximity of the receptor surface, limiting the accessible conformational space of interest. Such a procedure predicts binding modes and binding free energies, providing a canonical ensemble of the ligand–receptor system at each specific temperature considered and permitting the extraction of structural and energetic information on several ligand–receptor arrangements sampled. A cutoff parameter has been introduced in postproductive calculations in order to create a reference point suitable for measuring the free energy difference between bound and unbound states. The use of this parameter is a simple way to assess the decay of the ligand density probability around the receptor with the increase of the radial distance, which is, probably, directly related to what is experimentally detected in fluorescence or NMR titration. We assessed our methodology with a set of protein receptor–ligand test cases. In every case studied, the method was able to dock the ligand on the experimentally known receptor binding site and to calculate its binding free energy. The cutoff was kept constant at 3.5 Å for all five test cases, and it was possible to find a range of values that best interpolates the experimental data, though it was not guaranteed by different derivatives and intercepts of the curves reported in Figure S8.

However, this does not necessarily imply that the experimental ligand geometry is exactly predicted as prevalent binding mode. Instead, several binding modes are detected, which share the same binding region identified by experiments. This reflects that relatively large and rather flexible ligands may, at the binding site, adopt a huge plethora of orientations and conformations, especially when the receptor does not present a well-defined deep cleft as binding site but instead offers surface patches as binding regions. In particular, it was possible to collect and organize all arrangements according to their RMSD. Thus, a series of structural related conformations may be aggregated/classified to represent single binding modes. Each binding mode is characterized by its own dissociation constant and contributes differently to the overall binding affinity that is macroscopically measured between the ligand and the receptor.

It is worth noting that the configurations sampled during c-REMD simulations are absolutely independent of the cutoff used, because this parameter has not been introduced in this stage yet. Therefore, the distribution of the ligand around the receptor and on its surface is not determined by the use of the cutoff. Thus, we obtain a distribution of binding poses independently of the use of the cutoff. A binding mode is more populated with respect to another independently of the use of the cutoff, in the same way that a ligand is closer to a given receptor with respect to another system. Therefore, the free energy differences between two binding modes or two radial distributions are independent of the cutoff. It is not possible to adjust the cutoff in order to have the expected binding free energy associated with a single binding mode, better if with a small deviation from the experimental one, without significantly affect the total binding free energy. In addition, the fact that we obtain multiple binding poses, repeating the simulations using the experimental structures as starting configuration, reveals that alternative binding poses are actually possible according to the force field used and that they are sampled anyway.

The idea that a ligand may dock the receptor binding site using alternative arrangements is suggested also by other computational or experimental works.^{66–69} Obviously, such a structural disorder may be more marked and important in some systems than others, as shown, for example, when we have compared the WW systems. This suggests that in some cases each attempt to identify a single arrangement, which is responsible for the entire experimental binding affinity, may be a conundrum, especially if we face complex ligand–receptor systems, and points out on the importance in such cases of considering multiple binding modes, in order to obtain a good correspondence between structures and experimental binding affinities.

ASSOCIATED CONTENT

Supporting Information

Acceptance ratio statistics from replica exchange MD simulations. Snapshots depicting an unbound state and the initial configuration of the PDZ domain. Time series of temperatures, replica indices, root-mean-square deviations, and minimum distances between ligand and receptor from REMD simulation of PDZ. Plot of the binding free energy vs cutoff. Representative structures of the most populated clusters of the APSYSPPPPP p41 peptide bound to Spc SH3 domain (R21A mutant), of the GTPPPPYTVG peptide bound to the YAP65 WW domain (wild type and L30K mutant), of the SHRPPPP-GHR peptide bound to the CD2BP2 GYF domain. The Supporting Information is available free of charge on the ACS Publications website at DOI: [10.1021/acs.jctc.5b00253](https://doi.org/10.1021/acs.jctc.5b00253).

AUTHOR INFORMATION

Corresponding Authors

*Phone: 39.06.72594465. Fax: 39.06.72594328. E-mail: massimiliano.anselmi@uniroma2.it (M.A.). Corresponding author address: Dipartimento di Scienze e Tecnologie Chimiche, Università di Roma “Tor Vergata”, Via della Ricerca Scientifica, 00133 Rome, Italy.

*Phone: 49.(0)351.46340071. Fax: 49.(0)351.46340087. E-mail: mayte@biotec.tu-dresden.de (M.T.P.).

Author Contributions

The manuscript was written through contributions of all authors. All authors have given approval to the final version of the manuscript.

Notes

The authors declare no competing financial interest.

ACKNOWLEDGMENTS

The authors thank the ZIH TU Dresden for high-performance computational resources, Ralf Gey for technical assistance, and the members of the group for helpful discussions.

REFERENCES

- (1) Leach, A. R.; Shoichet, B. K.; Peishoff, C. E. Prediction of protein-ligand interactions. Docking and scoring: successes and gaps. *J. Med. Chem.* **2006**, *49*, 5851–5855.
- (2) Moitessier, N.; Englebienne, P.; Lee, D.; Lawandi, J.; Corbeil, C. R. Towards the development of universal, fast and highly accurate docking/scoring methods: a long way to go. *Biophys. Rev.* **2008**, *153* (Suppl 1), S7–S26.
- (3) Moal, I. H.; Moretti, R.; Baker, D.; Fernandez-Recio, J. Scoring functions for protein-protein interactions. *Curr. Opin. Struct. Biol.* **2013**, *23*, 862–867.
- (4) Wang, J. C.; Lin, J. H. Scoring functions for prediction of protein-ligand interactions. *Curr. Pharm. Des.* **2013**, *19*, 2174–2182.
- (5) Claussen, H.; Buning, C.; Rarey, M.; Lengauer, T. FlexE: efficient molecular docking considering protein structure variations. *J. Mol. Biol.* **2001**, *308*, 377–395.
- (6) Sherman, W.; Day, T.; Jacobson, M. P.; Friesner, R. A.; Farid, R. Novel procedure for modeling ligand/receptor induced fit effects. *J. Med. Chem.* **2006**, *49*, 534–553.
- (7) Bolia, A.; Gerek, Z. N.; Ozkan, S. B. BP-Dock: a flexible docking scheme for exploring protein-ligand interactions based on unbound structures. *J. Chem. Inf. Model.* **2014**, *54*, 913–925.
- (8) Durrant, J. D.; McCammon, J. A. Computer-aided drug-discovery techniques that account for receptor flexibility. *Curr. Opin. Pharmacol.* **2010**, *10*, 770–774.
- (9) Fischer, M.; Coleman, R. G.; Fraser, J. S.; Shoichet, B. K. Incorporation of protein flexibility and conformational energy penalties in docking screens to improve ligand discovery. *Nat. Chem.* **2014**, *6*, 575–583.
- (10) Wang, J.; Dixon, R.; Kollman, P. A. Ranking ligand binding affinities with avidin: a molecular dynamics-based interaction energy study. *Proteins: Struct., Funct., Genet.* **1999**, *34*, 69–81.
- (11) Bash, P. A.; Singh, U. C.; Brown, F. K.; Langridge, R.; Kollman, P. A. Calculation of the relative change in binding free energy of a protein-inhibitor complex. *Science* **1987**, *235*, 574–576.
- (12) Bash, P. A.; Singh, U. C.; Langridge, R.; Kollman, P. A. Free energy calculations by computer simulation. *Science* **1987**, *236*, 564–568.
- (13) Beveridge, D. L.; Di Capua, F. M. In *Computer Simulation of Biomolecular Systems*; Van Gunsteren, W. F., Weiner, P. K., Eds.; ESCOM: Leiden, 1989; pp 1–26.
- (14) Sneddon, S. F.; Tobias, D. J.; Brooks, C. L., 3rd Thermodynamics of amide hydrogen bond formation in polar and apolar solvents. *J. Mol. Biol.* **1989**, *209*, 817–820.
- (15) Aqvist, J. Calculation of absolute binding free energies for charged ligands and effects of long-range electrostatic interactions. *J. Comput. Chem.* **1996**, *17*, 1587–1597.
- (16) Aqvist, J.; Hansson, T. On the validity of electrostatic linear response in polar solvents. *J. Phys. Chem.* **1996**, *100*, 9512–9521.
- (17) Hansson, T.; Aqvist, J. Estimation of binding free energies for hiv proteinase inhibitors by molecular dynamics simulations. *Protein Eng., Des. Sel.* **1995**, *8*, 1137–1144.
- (18) Aqvist, J.; Medina, C.; Samuelsson, J. E. New method for predicting binding affinity in computer-aided drug design. *Protein Eng., Des. Sel.* **1994**, *7*, 385–391.
- (19) Swanson, J. M.; Henchman, R. H.; McCammon, J. A. Revisiting free energy calculations: a theoretical connection to MM/PBSA and direct calculation of the association free energy. *Biophys. J.* **2004**, *86*, 67–74.
- (20) Kumar, S.; Bouzida, D.; Swendsen, S. H.; Kollman, P. A.; Rosenberg, J. M. The Weighted Histogram Analysis Method for free-energy calculations on biomolecules. I. the method. *J. Comput. Chem.* **1992**, *13*, 1011–1021.
- (21) Grubmuller, H. Force probe molecular dynamics simulations. *Methods Mol. Biol.* **2005**, *305*, 493–515.
- (22) Samsonov, S. A.; Gehrcke, J. P.; Pisabarro, M. T. Flexibility and explicit solvent in molecular-dynamics-based docking of protein-glycosaminoglycan systems. *J. Chem. Inf. Model.* **2014**, *54*, 582–592.
- (23) Di Nola, A.; Roccatano, D.; Berendsen, H. J. Molecular dynamics simulation of the docking of substrates to proteins. *Proteins: Struct., Funct., Genet.* **1994**, *19*, 174–182.
- (24) Mangoni, M.; Roccatano, D.; Di Nola, A. Docking of flexible ligands to flexible receptors in solution by molecular dynamics simulation. *Proteins: Struct., Funct., Genet.* **1999**, *35*, 153–162.
- (25) Pak, Y.; Wang, S. Application of a molecular dynamics simulation method with a generalized effective potential to the flexible molecular docking problems. *J. Phys. Chem. B* **2000**, *104*, 354–359.
- (26) Nakajima, N.; Higo, J.; Kidera, A.; Nakamura, H. Flexible docking of a ligand peptide to a receptor protein by multicanonical molecular dynamics simulation. *Chem. Phys. Lett.* **1997**, *278*, 297–301.
- (27) Merlitz, H.; Wenzel, W. Comparison of stochastic optimization methods for receptor–ligand docking. *Chem. Phys. Lett.* **2002**, *362*, 271–277.
- (28) Merlitz, H.; Burghardt, B.; Wenzel, W. Application of the stochastic tunneling method to high throughput database screening. *Chem. Phys. Lett.* **2003**, *370*, 68–73.
- (29) Fukunishi, Y.; Mikami, Y.; Nakamura, H. The Filling Potential method: a method for estimating the free energy surface for protein-ligand docking. *J. Phys. Chem. B* **2003**, *107*, 13201–13210.
- (30) Cvijovic, D.; Klinowski, J. Taboo search: an approach to the multiple minima problem. *Science* **1995**, *267*, 664–666.
- (31) Gervasio, F. L.; Laio, A.; Parrinello, M. Flexible docking in solution using metadynamics. *J. Am. Chem. Soc.* **2005**, *127*, 2600–2607.
- (32) Sugita, Y.; Okamoto, Y. Replica-exchange molecular dynamics method for protein folding. *Chem. Phys. Lett.* **1999**, *314*, 141–151.
- (33) Atkovska, K.; Samsonov, S. A.; Paszkowski-Rogacz, M.; Pisabarro, M. T. Multipole binding in molecular docking. *Int. J. Mol. Sci.* **2014**, *15*, 2622–2645.
- (34) Guedes, I. A.; de Magalhaes, C. S.; Dardenne, L. E. Receptor–ligand molecular docking. *Biophys. Rev.* **2014**, *6*, 75–87.
- (35) Laio, A.; Parrinello, M. Escaping free-energy minima. *Proc. Natl. Acad. Sci. U. S. A.* **2002**, *99*, 12562–12566.
- (36) Mezei, M. A new method for mapping macromolecular topography. *J. Mol. Graphics Modell.* **2003**, *21*, 463–472.
- (37) Casares, S.; Ab, E.; Eshuis, H.; Lopez-Mayorga, O.; van Nuland, N. A.; Conejero-Lara, F. The high-resolution NMR structure of the R21A Spe-SH3:P41 complex: understanding the determinants of binding affinity by comparison with Abl-SH3. *BMC Struct. Biol.* **2007**, *7*, 22.
- (38) Pires, J. R.; Taha-Nejad, F.; Toepert, F.; Ast, T.; Hoffmuller, U.; Schneider-Mergener, J.; Kuhne, R.; Macias, M. J.; Oschkinat, H. Solution structures of the YAP65 WW domain and the variant L30 K in complex with the peptides GTTPPPPYTVG, N-(n-octyl)-GPPPY and PLPPY and the application of peptide libraries reveal a minimal binding epitope. *J. Mol. Biol.* **2001**, *314*, 1147–1156.
- (39) Skelton, N. J.; Koehler, M. F.; Zobel, K.; Wong, W. L.; Yeh, S.; Pisabarro, M. T.; Yin, J. P.; Lasky, L. A.; Sidhu, S. S. Origins of PDZ domain ligand specificity. Structure determination and mutagenesis of the Erbin PDZ domain. *J. Biol. Chem.* **2003**, *278*, 7645–7654.
- (40) Freund, C.; Kuhne, R.; Yang, H.; Park, S.; Reinherz, E. L.; Wagner, G. Dynamic interaction of CD2 with the GYF and the SH3 domain of compartmentalized effector molecules. *EMBO J.* **2002**, *21*, 5985–5995.

- (41) Gmeiner, W. H.; Horita, D. A. Implications of SH3 domain structure and dynamics for protein regulation and drug design. *Cell Biochem. Biophys.* **2001**, *35*, 127–140.
- (42) Kay, B. K.; Williamson, M. P.; Sudol, M. The importance of being proline: the interaction of proline-rich motifs in signaling proteins with their cognate domains. *FASEB J.* **2000**, *14*, 231–241.
- (43) Mayer, B. J. SH3 domains: complexity in moderation. *J. Cell. Sci.* **2001**, *114*, 1253–1263.
- (44) Pisabarro, M. T.; Serrano, L. Rational design of specific high-affinity peptide ligands for the Abl-SH3 domain. *Biochemistry* **1996**, *35*, 10634–10640.
- (45) Viguera, A. R.; Arondo, J. L.; Musacchio, A.; Saraste, M.; Serrano, L. Characterization of the interaction of natural proline-rich peptides with five different SH3 domains. *Biochemistry* **1994**, *33*, 10925–10933.
- (46) Bork, P.; Sudol, M. The WW domain: a signalling site in dystrophin? *Trends Biochem. Sci.* **1994**, *19*, 531–533.
- (47) Andre, B.; Springael, J. Y. WWP, a new amino acid motif present in single or multiple copies in various proteins including dystrophin and the SH3-binding Yes-associated protein YAP65. *Biochem. Biophys. Res. Commun.* **1994**, *205*, 1201–1205.
- (48) Hofmann, K.; Bucher, P. The rsp5-domain is shared by proteins of diverse functions. *FEBS Lett.* **1995**, *358*, 153–157.
- (49) Chen, H. I.; Sudol, M. The WW domain of Yes-associated protein binds a proline-rich ligand that differs from the consensus established for Src homology 3-binding modules. *Proc. Natl. Acad. Sci. U. S. A.* **1995**, *92*, 7819–7823.
- (50) Cho, K. O.; Hunt, C. A.; Kennedy, M. B. The rat brain postsynaptic density fraction contains a homolog of the Drosophila discs-large tumor suppressor protein. *Neuron* **1992**, *9*, 929–942.
- (51) Kim, E.; Niethammer, M.; Rothschild, A.; Jan, Y. N.; Sheng, M. Clustering of Shaker-type K⁺ channels by interaction with a family of membrane-associated guanylate kinases. *Nature* **1995**, *378*, 85–88.
- (52) Woods, D. F.; Bryant, P. J. ZO-1, DlgA and PSD-95/SAP90: homologous proteins in tight, septate and synaptic cell junctions. *Mech. Dev.* **1993**, *44*, 85–89.
- (53) Morais Cabral, J. H.; Petosa, C.; Sutcliffe, M. J.; Raza, S.; Byron, O.; Poy, F.; Marfatia, S. M.; Chishti, A. H.; Liddington, R. C. Crystal structure of a PDZ domain. *Nature* **1996**, *382*, 649–652.
- (54) Hess, B.; Kutzner, C.; van Der Spoel, D.; Lindahl, E. GROMACS 4: Algorithms for Highly Efficient, Load-Balanced, and Scalable Molecular Simulation. *J. Chem. Theory Comput.* **2008**, *4*, 435–447.
- (55) Duan, Y.; Wu, C.; Chowdhury, S.; Lee, M. C.; Xiong, G.; Zhang, W.; Yang, R.; Cieplak, P.; Luo, R.; Lee, T.; Caldwell, J.; Wang, J.; Kollman, P. A point-charge force field for molecular mechanics simulations of proteins based on condensed-phase quantum mechanical calculations. *J. Comput. Chem.* **2003**, *24*, 1999–2012.
- (56) Hess, B. P-LINCS: A Parallel Linear Constraint Solver for Molecular Simulation. *J. Chem. Theory Comput.* **2008**, *4*, 116–122.
- (57) Bussi, G.; Donadio, D.; Parrinello, M. Canonical sampling through velocity rescaling. *J. Chem. Phys.* **2007**, *126*, 014101.
- (58) Qui, D.; Shenkin, P.; Hollinger, F.; Still, W. The GB/SA continuum model for solvation. A fast analytical method for the calculation of approximate Born radii. *J. Phys. Chem. A* **1997**, *101*, 3005–3014.
- (59) Patriksson, A.; van der Spoel, D. A temperature predictor for parallel tempering simulations. *Phys. Chem. Chem. Phys.* **2008**, *10*, 2073–2077.
- (60) Macias, M. J.; Hyvonen, M.; Baraldi, E.; Schultz, J.; Sudol, M.; Saraste, M.; Oschkinat, H. Structure of the WW domain of a kinase-associated protein complexed with a proline-rich peptide. *Nature* **1996**, *382*, 646–649.
- (61) Kofler, M. M.; Freund, C. The GYF domain. *FEBS J.* **2006**, *273*, 245–256.
- (62) Gerek, Z. N.; Ozkan, S. B. A flexible docking scheme to explore the binding selectivity of PDZ domains. *Protein Sci.* **2010**, *19*, 914–928.
- (63) Niv, M. Y.; Weinstein, H. A flexible docking procedure for the exploration of peptide binding selectivity to known structures and homology models of PDZ domains. *J. Am. Chem. Soc.* **2005**, *127*, 14072–14079.
- (64) Meiler, J.; Baker, D. ROSETTALIGAND: protein-small molecule docking with full side-chain flexibility. *Proteins: Struct., Funct., Genet.* **2006**, *65*, 538–548.
- (65) Gohlke, H.; Hendlich, M.; Klebe, G. Knowledge-based scoring function to predict protein-ligand interactions. *J. Mol. Biol.* **2000**, *295*, 337–356.
- (66) Kallblad, P.; Mancera, R. L.; Todorov, N. P. Assessment of multiple binding modes in ligand-protein docking. *J. Med. Chem.* **2004**, *47*, 3334–3337.
- (67) Stjernschantz, E.; Oostenbrink, C. Improved ligand-protein binding affinity predictions using multiple binding modes. *Biophys. J.* **2010**, *98*, 2682–2691.
- (68) Feng, S.; Chen, J. K.; Yu, H.; Simon, J. A.; Schreiber, S. L. Two binding orientations for peptides to the Src SH3 domain: development of a general model for SH3-ligand interactions. *Science* **1994**, *266*, 1241–1247.
- (69) Lewi, P. J.; de Jonge, M.; Daeyaert, F.; Koymans, L.; Vinkers, M.; Heeres, J.; Janssen, P. A.; Arnold, E.; Das, K.; Clark, A. D., Jr.; Hughes, S. H.; Boyer, P. L.; de Bethune, M. P.; Pauwels, R.; Andries, K.; Kukla, M.; Ludovici, D.; De Corte, B.; Kavash, R.; Ho, C. On the detection of multiple-binding modes of ligands to proteins, from biological, structural, and modeling data. *J. Comput.-Aided Mol. Des.* **2003**, *17*, 129–134.